Received: 29 February 2024 | Revised: 27 May 2024 | Accepted: 30 May 2024

DOI: 10.1002/pro.5079

THE PROTEIN SOCIETY WILEY

RESEARCH NOTE

# Conformational diversity of human HP1α

**Tina Ukmar-Godec**[1] | **Taekyung Yu**[1] | **Alain Ibanez de Opakua**[1] | **Christian F. Pantoja**[1] | **Francesca Munari**[2] | **Markus Zweckstetter**[1,3]

[1]German Center for Neurodegenerative Diseases (DZNE), Translational Structural Biology, Göttingen, Germany

[2]Department of Biotechnology, University of Verona, Verona, Italy

[3]Department of NMR-based Structural Biology, Max Planck Institute for Multidisciplinary Sciences, Göttingen, Germany

**Correspondence**
Markus Zweckstetter, German Center for Neurodegenerative Diseases (DZNE), Translational Structural Biology, Von-Siebold-Str. 3a, 37075 Göttingen, Germany.
Email: Markus.Zweckstetter@dzne.de

**Funding information**
European Research Council, Grant/Award Number: 787679

**Review Editor:** Carol Beth Post

## Abstract

Heterochromatin protein 1 alpha (HP1α) is an evolutionarily conserved protein that binds chromatin and is important for gene silencing. The protein comprises 191 residues arranged into three disordered regions and two structured domains, the chromo and chromoshadow domain, which associates into a homodimer. While high-resolution structures of the isolated domains of HP1 proteins are known, the structural properties of full-length HP1α remain largely unknown. Using a combination of NMR spectroscopy and structure predictions by AlphaFold2 we provide evidence that the chromo and chromoshadow domain of HP1α engage in direct contacts resulting in a compact chromo/chromoshadow domain arrangement. We further show that HP1β and HP1γ have increased interdomain dynamics when compared to HP1α which may contribute to the distinct roles of different Hp1 isoforms in gene silencing and activation.

**KEYWORDS**

AlphaFold, chromatin, dynamics, HP1α, NMR spectroscopy, residual dipolar couplings

## 1 | INTRODUCTION

Mammalian genomes encode three HP1 isoforms, namely HP1α, HP1β, and HP1γ (Jones et al., 2000; Zeng et al., 2010), displaying distinct subnuclear localizations and playing specific roles in heterochromatin structure and organization (Bosch-Presegue et al., 2017). HP1α is commonly associated with gene silencing whereas HP1β and HP1γ have both gene-silencing and gene-activating roles (Bosch-Presegue et al., 2017; Vakoc et al., 2005). HP1 proteins show a multi-domain organization in the form of two globular domains called chromodomain (CD) and the chromoshadow domain (CSD) that are connected via a long weakly conserved hinge region (HR) and along at the respective ends with highly charged unstructured N- and C-terminal tails (NTE and CTE) (Eissenberg and Elgin, 2000) (Figure 1a,b). Hp1 proteins exist as dimers mediated by CD-CSD interactions (Figure 1a).

The molecular origin of the distinctive functions of α and β and γ isoforms of HP1 remains poorly understood. The less conserved and less ordered HR and N-, and C-terminal domains, whose electrostatic properties vary markedly between the isoforms, are hypothesized to be responsible for their distinct modes of action as a result of differences in DNA binding (Bryan et al., 2017; Kilic et al., 2015; Mishima et al., 2013; Nishibuchi et al., 2014; Smothers and Henikoff, 2001). By comparing the three HP1 isoforms, HP1α exhibits the longest residence times and fastest binding rates on

H3K9-methylated chromatin (Bryan et al., 2017). Additionally, all three isoforms display a two-stage dissociation form H3K9-methylated chromatin, implying two distinct subpopulations of bound HP1 (Bryan et al., 2017). HP1α may attain a closed compact form that could contribute to HP1α's role in chromatin compaction (Larson et al., 2017). Further extending the structural landscape of HP1 proteins, yeast HP1α was observed to oligomerize via CD–CD interactions (Canzio et al., 2011) whereas no CD–CD interactions were observed in human HP1β (Munari et al., 2012). Despite these advances, the molecular mechanisms responsible for the discriminatory mode of action of different HP1 isoforms remain largely unknown.

To gain a better understanding of the structural and dynamical properties of human full-length HP1α, we combined NMR spectroscopy, in particular residual dipolar couplings (RDCs) (Jung and Zweckstetter, 2004; Lipsitz and Tjandra, 2004; Zweckstetter and Bax, 2002), which provide long-range orientational information, with predictions by the neural network-based method AlphaFold2 (Jumper et al., 2021; Varadi et al., 2022). Our studies support differences in interdomain dynamics between the three HP1 isoforms.

## 2 | RESULTS AND DISCUSSION

To gain insight into the structural properties of human full-length HP1α, we recombinantly produced $^{2}H/^{13}C/^{15}N$-labeled protein and analyzed it using multidimensional NMR spectroscopy. On the basis of the sequence-specific assignment (Ukmar-Godec et al., 2023), we predicted the protein's residue-specific secondary-structure propensity using TALOS N+ (Shen et al., 2009). Secondary structure propensities predicted by TALOS N+ are in agreement with the high-resolution structures of the individual CD and CSD, and suggested the presence of predominantly random coil conformation in the NTE, the HR, and the CTE (Figure 1c). However, three non-globular regions display structural bias in solution (>10%): residue 3–10 in the NTE favors extended β-structure-like conformations, while residue 99–110 in the HR and residue 179–190 in the CTE transiently populate α-helical structure (Figure 1d).

To characterize the relative orientation of the CD and CSD in full-length HP1α, we measured $^{1}H$-$^{15}N$ RDCs (Figure S1 in Data S1) (Jung and Zweckstetter, 2004; Zweckstetter and Bax, 2002). The experimental RDCs correlated well with the values back-calculated from crystal structures of the individual domains with Pearson's

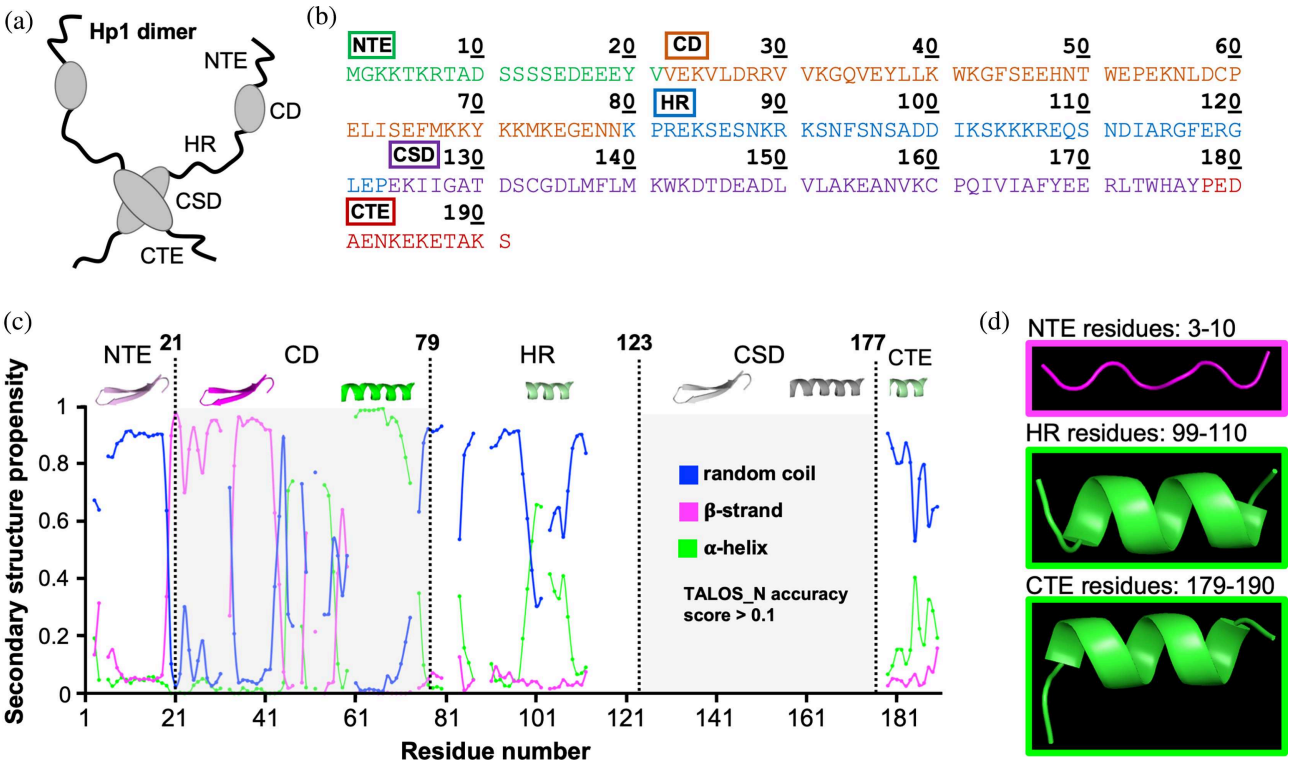


**FIGURE 1** Structural properties of human full-length HP1α. (a) Schematic of Hp1 dimer containing the ordered CD and CSD and disordered NTE, HR, and CTE. (b) Amino acid sequence of HP1α. (c) Residue-specific secondary structure propensity determined by TALOS N+ on the basis of the experimental NMR assignments of full-length HP1α. (d) Generated model conformations of transient structures in the NTE, HR, and CTE of HP1α. CD, chromodomain; CSD, chromoshadow domain; HR, hinge region.

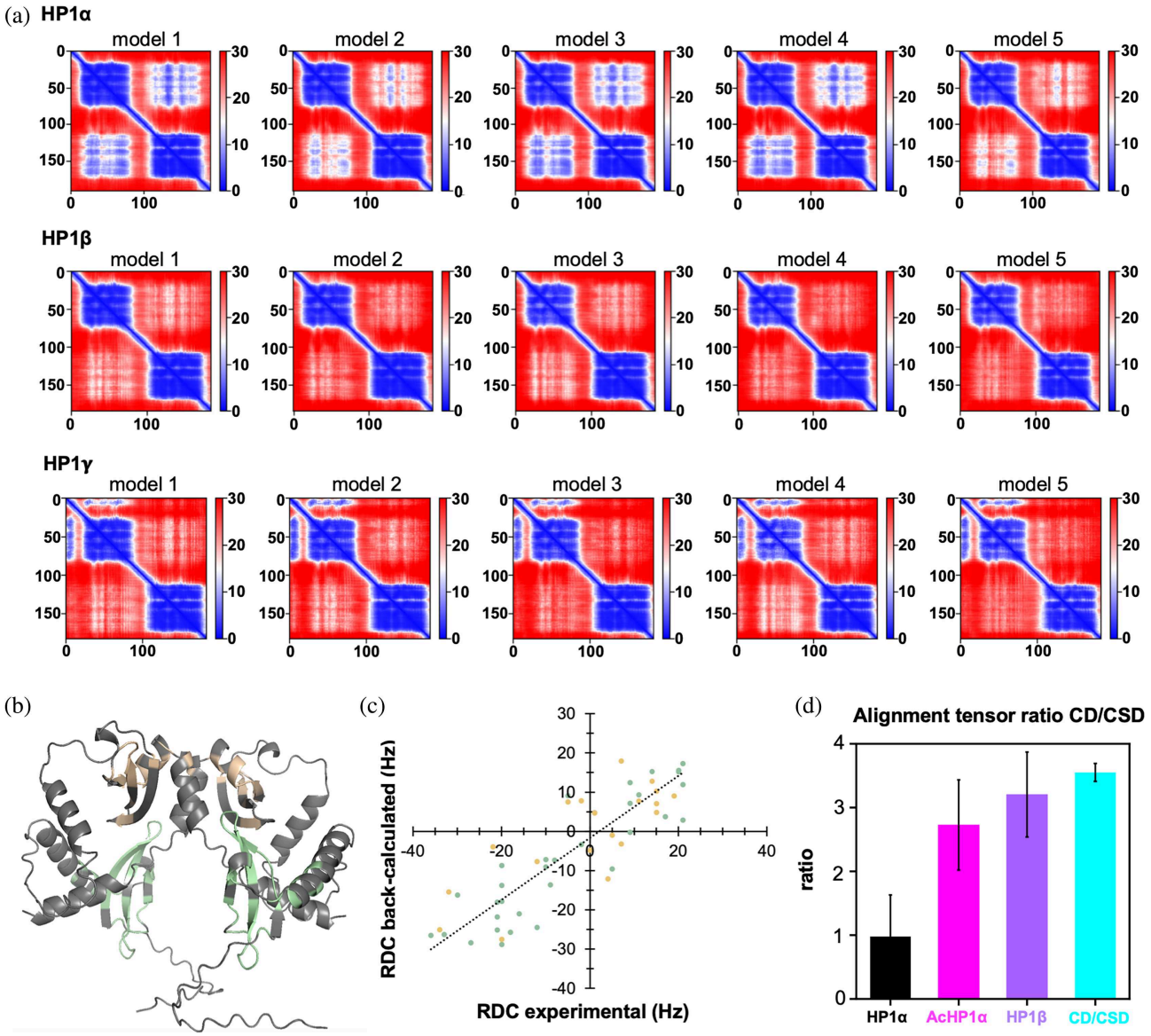


**FIGURE 2** HP1α CD/CSD arrangement differs from HP1β and HP1γ. (a) Aligned errors for five model structures predicted by AlphaFold2 for HP1α (top), HP1β (middle), and HP1γ (bottom). The color at position (*x*, *y*) indicates AlphaFold2's expected position error at residue *x*, when the predicted and true structures are aligned on residue *y*. (b) HP1α dimer model predicted by the multimer model of AlphaFold2 (Jumper et al., 2021; Mirdita et al., 2022); residues highlighted in green (CD) and orange (CSD) were used for RDC analysis (see Figure 2c). (c) Correlation between experimental $^{1}H$-$^{15}N$ RDCs and RDCs back-calculated from the AlphaFold2-predicted 3D structure of the HP1α dimer shown in (b). (d) Ratios of the RDC-derived alignment tensor magnitudes Da(HN) between the CD and the CSD, that is, $Da(HN)^{CD}/Da(HN)^{CSD}$, in full-length HP1α (black), AcHP1α (magenta), and HP1β (violet). For comparison, the CSD/CD ratio of alignment magnitudes predicted by PALES for the individual CSD and CD domains of HP1α and HP1β are shown in cyan. Error bars represent std. CD, chromodomain; CSD, chromoshadow domain; RDC, residual dipolar coupling.

correlation coefficients of 0.96 and 0.97, respectively (Table S1 in Data S1). The analysis confirms that the structures of the two globular domains in solution and in the crystal are highly similar, and that the accuracy of the experimental RDCs is high (Figure S2a in Data S1). Comparison of the parameters of the alignment tensors best-fitted to the crystal structures of the CD and CSD further showed that the derived magnitude and rhombicity are identical for the two domains within experimental errors (Table S1 in Data S1). The orientation of the major axes of the alignment tensors of the CD and CSD are however not identical (Figure S2d in Data S1).

To obtain insight into structural models of full-length HP1α, we next performed AlphaFold2 predictions (Jumper et al., 2021; Mirdita et al., 2022) (Figure S3 in

Data S1). AlphaFold2 predicts the CD and CSD to be in direct contact (Figure S3 in Data S1), with evolutionary contacts connecting the two domains (Figure 2a and Figure S4 in Data S1). The CD-CSD contacts broadly cover the sequences of the CD and CSD such that no unique relative domain orientation was attained (Figure S3 in Data S1). We thus used the RDC values to probe which of the five predicted, monomeric AlphaFold2-models best fit to the experimental NMR measurements of HP1α. To this end we simultaneously fitted the 52 RDCs of both the CD and CSD to the five AlphaFold2-models using singular value decomposition. A high correlation between the experimental and back-calculated RDCs suggests that the relative domain orientation seen in a structural model is a good representation of the solution conformation. The analysis resulted in correlations of ∼0.7 between experimental and back-calculated RDCs for three AlphaFold2-models (Figure S3 in Data S1). In case the relative domain orientation between the two domains would perfectly represent the solution conformation, we would expect a correlation of 0.9–0.96, that is, matching that of the RDC fit to the individual domains.

We also predicted dimer models of HP1α using AlphaFold2 (Figure 2b and Figure S5 in Data S1, Model 4). In all five dimer models, the CD and CSD are in direct contact (Figure S5a in Data S1). For the dimer model best in agreement with the experimental RDCs, the correlation between predicted and back-calculated RDCs is 0.86 (Figure S5b in Data S1). The higher RDC correlation of the dimeric Model 4 when compared to any monomeric AlphaFold2-predicted model is due to a slightly different relative domain orientation in the dimeric Model 4 structure. Notably, the correlation of 0.86 is already very high considering that all 52 RDCs from both domains were used during singular value decomposition. The decrease in RDC correlation when compared to the fit to the individual domains may arise from inaccuracies in the relative domain orientation or the presence of a dynamic exchange between a closed and an open conformation.

We then asked whether the compact CD/CSD conformation is specific for HP1α. To address this question, we acetylated HP1α in vitro using CREB/p300 and recorded the $^{1}$H-$^{15}$N RDCs of acetylated HP1α (AcHP1α). Previous studies showed that CREB/p300 acetylates K3, K6, K42, and K91 of HP1α and thus removes four positive charges: two positive charges (K3 and K6) in the NTE, one positive charge (K42) in the CD, and one positive charge (K91) in the HR (Ukmar-Godec et al., 2023). Although the concentration of acetylated HP1α was lower than its non-acetylated form increasing the experimental measurement error, good fits of the RDCs of the CD and CSD to the individual CD and CSD were obtained (Figure S2b and Table S1 in Data S1). Comparison of the alignment tensor parameters between unmodified and acetylated HP1α reveals two notable differences: the rhombicity of the alignment tensors changes from more axially symmetric to more rhombic upon acetylation, and the magnitude of the alignment tensor of the CSD is ∼2.7-fold larger when compared to the CD in the acetylated protein (Figure 2d). In contrast, the CD and CSD have the same alignment tensor magnitude (within experimental errors) in unmodified HP1α, an RDC property expected for domains that reorient in solution together, or where different motional order parameters of the two domains lead to the same alignment tensor magnitude (Figure 2d and Table S1 in Data S1). The RDC analysis suggests that the overall structure of full-length HP1α changes with the CD and CSD becoming decoupled upon HP1α acetylation.

We next recombinantly produced HP1β and recorded its $^{1}$H-$^{15}$N RDCs. The RDC fits to the high-resolution structures of the CD and CSD are comparable to the fits obtained for HP1α (Figure S2c and Table S1 in Data S1). The alignment tensors derived for the CD and CSD of HP1β have low rhombicity, as in unmodified HP1α. In contrast to HP1α, however, the alignment tensor magnitudes strongly differ between the CD and CSD of HP1β: the CSD aligns ∼3.2 times stronger than the CD (Figure 2d and Table S1 in Data S1). The strong difference in alignment indicates that the two domains are decoupled in HP1β such that they reorient independently in solution. The stronger alignment of the CSD when compared to the CD is further in agreement with a more anisotropic shape of the CSD dimer when compared to the CD monomer. Additional analyses of the alignment tensor, predicted by the software PALES on the basis of the isolated structures of the two domains, CD and CSD, revealed that the alignment tensor ratio of the isolated CD and CSD is ∼3.5, which is in good agreement with the experimental alignment magnitudes of the two domains in the decoupled state of the studied proteins (Figure 2d and Table S2 in Data S1).

The RDC analysis indicates that the CD and CSD of HP1α engage in direct contacts. Consistent with this interpretation, AlphaFold2 predicts interactions between the two domains (Figure 2a and Figure S4 in Data S1). Previously, small angle x-ray scattering (SAXS) together with size-exclusion chromatography coupled to multi-angle light scattering suggested that unmodified HP1α may attain an overall compact conformation ($D_{max}$ ≈ 13 nm) that becomes extended ($D_{max}$ ≈ 22 nm) upon phosphorylation of HP1α (Larson et al., 2017). SAXS experiments of HP1β, on the other hand, revealed that HP1β populate a wide conformational space of more elongated structures ($D_{max}$ ≈ 16 nm) (Munari et al., 2013).

Consistent with these studies, AlphaFold2 predicts less contacts between the CD and CSD of HP1β where the NMR analysis shows that the two domains reorient largely independent from each other in solution. AlphaFold2 also predicts less CD-CSD interactions in HP1γ when compared to HP1α (Figure 2a), which supports coarse-grained simulations predicting a large radius of gyration of HP1γ (3.48 ± 0.69 nm) relative to HP1α (3.20 ± 0.31 nm) (Phan et al., 2023). The combined data suggest that interactions between the CD and CSD are evolutionary favored in HP1α when compared to HP1β and HP1γ. Notably, all three HP1 isoforms have very similar amino acid sequences in the CD and the CSD (Figure S6a,b in Data S1). However, small differences in the amino acid sequences of the CD result in a change in the electrostatic properties of the CD of HP1α when compared to HP1β and HP1γ with pI values of 6.8, 4.7, and 4.4 for HP1α, HP1β, and HP1γ, respectively (Figure S6b in Data S1).

The AlphaFold2-predicted structural model displayed in Figure 2b is one possible arrangement which the CD and CSD may assume in HP1α. However, other relative orientations may also be possible (Figure S5 in Data S1), and the disordered regions, especially the HR which is substantially more positively charged in HP1α (pI ∼ 10) than in HP1β (pI ∼ 8) (see Figure S6b in Data S1), may interact with each other, and/or transiently bind to either the CD or CSD. Additionally, HP1α may populate an ensemble of closed conformations resembling those shown in Figure 2b in equilibrium with more open conformations, that is, that HP1α, HP1β, and HP1γ differ in the population of closed and open conformations and thus in interdomain dynamics. Such isoform-specific differences in interdomain dynamics may be associated with their distinct roles in gene silencing and activation (Bosch-Presegue et al., 2017; Vakoc et al., 2005).

## 3 | MATERIALS AND METHODS

### 3.1 | Expression and purification of recombinant Hp1 proteins

HP1α (UniProt number P45973) was expressed in *Escherichia coli* strain BL21 (DE3) from a pET15b vector (please see Ukmar-Godec et al., 2023). $^{15}$N-perdeutereted HP1α was expressed in $D_2O$-based minimal medium, using $^{15}NH_4Cl$ and $^{2}H$, $^{12}C$-glucose as unique source of nitrogen. The expression and purification protocol is explained in detail in Ukmar-Godec et al. (2023). $^{15}$N-perdeutereted HP1β (UniProt number P83916) was expressed and purified according to previously published protocols (Munari et al., 2012). Protein concentrations were determined by Nanodrop and flash-frozen aliquots were stored at −80°C.

### 3.2 | Protein acetylation

HP1α was acetylated using CREB (recombinant hCREB binding protein) and p300 according to previously published protocols (Ukmar-Godec et al., 2023).

### 3.3 | NMR spectroscopy

NMR spectra for the backbone assignment of human full-length HP1α were acquired at 303 K on a 900 MHz Brucker spectrometer (for details please see Ukmar-Godec et al., 2023). Residue-specific secondary structure propensities were calculated based on $^{13}C$-$^{15}N$ HP1α backbone resonance assignments using TALOS+ (Shen et al., 2009). To generate model conformations of the transient structures in the NTE, HR, and CTE from the NMR chemical shifts, phi and psi dihedral angles calculated by TALOS+ were applied using PyMOL version 2.1 (The PyMOL Molecular Graphics System) to a peptide with the corresponding HP1α sequence.

RDCs of HP1α and AcHP1α were determined using a 2D $^{1}H$-$^{15}N$ IPAP (In-Phase, Anti-Phase)-HSQC-based Bruker pulse program recorded at 303 K on a Bruker 800 MHz equipped with triple-resonance 5 mm cryogenic probe. For isotropic conditions, 150 μM $^{15}$N-perdeuterated HP1α and 50 μM $^{15}$N-perdeuterated AcHP1α in 20 mM MES (pH 6.2), 100 mM NaCl, 1 mM TCEP, and 10% $D_2O$ were used. Anisotropic conditions were achieved through addition of a 5% of pentaethylene glycol monododecyl ether (C12E5) and *n*-hexanol mixture resulting in 27.3 Hz and 24.5 Hz of quadrupolar splitting for HP1α and AcHP1α, respectively. For anisotropic conditions the salt concentration was reduced to 20 mM NaCl and the protein concertation to 50 μM. The RDCs of Hp1β were obtained as described in Munari et al. (2013). Shortly, the RDCs of Hp1β were measured using a TROSY-HSQC interleaved experiment recorded on a Bruker 900 MHz at 293 K equipped with a cryoprobe (Munari et al., 2013). Here, for isotropic conditions 200 μM $^{15}$N-perdeuterated HP1β in 20 mM NaP (pH 6.5), 50 mM NaCl, 2 mM DTT, 0.02% $NaN_3$, and 10% $D_2O$ were used. Anisotropic conditions were achieved same as with the other two protein, with 5% C12E5/hexanol resulting in 16 Hz of quadrupolar splitting. RDC data were analyzed using the PALES software (Zweckstetter, 2008). Crystal structures of the Hp1α CD (PDB code: 3fdt) and Hp1α CSD (PDB code: 3i3c, chain A), as well as

the simulated AlphaFold2 structures were visualized using PyMOL.

## AUTHOR CONTRIBUTIONS

**Tina Ukmar-Godec:** Investigation; formal analysis; visualization; writing – original draft; writing – review and editing. **Taekyung Yu:** Formal analysis. **Alain Ibanez de Opakua:** Formal analysis. **Christian F. Pantoja:** Formal analysis. **Francesca Munari:** Resources; writing – review and editing. **Markus Zweckstetter:** Conceptualization; funding acquisition; resources; formal analysis; supervision; writing – original draft; writing – review and editing.

## ACKNOWLEDGMENTS

We thank Irina Lushpinskaya for the advice on RDC sample preparation. M.Z. was supported by the European Research Council (ERC) under the EU Horizon 2020 research and innovation program (grant agreement no. 787679). Open Access funding enabled and organized by Projekt DEAL.

## CONFLICT OF INTEREST STATEMENT

The authors declare no conflicts of interest.

## DATA AVAILABILITY STATEMENT

The experimentally measured RDCs of the investigated proteins in this paper are included in the Supporting Data Sheet in Data S2.

## ORCID

*Tina Ukmar-Godec* https://orcid.org/0000-0002-5763-2856

## REFERENCES

Bosch-Presegue L, Raurell-Vila H, Thackray JK, Gonzalez J, Casal C, Kane-Goldsmith N, et al. Mammalian HP1 isoforms have specific roles in heterochromatin structure and organization. Cell Rep. 2017;21(8):2048–57.

Bryan LC, Weilandt DR, Bachmann AL, Kilic S, Lechner CC, Odermatt PD, et al. Single-molecule kinetic analysis of HP1-chromatin binding reveals a dynamic network of histone modification and DNA interactions. Nucleic Acids Res. 2017; 45(18):10504–17.

Canzio D, Chang EY, Shankar S, Kuchenbecker KM, Simon MD, Madhani HD, et al. Chromodomain-mediated oligomerization of HP1 suggests a nucleosome-bridging mechanism for heterochromatin assembly. Mol Cell. 2011;41(1):67–81.

Eissenberg JC, Elgin SC. The HP1 protein family: getting a grip on chromatin. Curr Opin Genet Dev. 2000;10(2):204–10.

Jones DO, Cowell IG, Singh PB. Mammalian chromodomain proteins: their role in genome organisation and expression. Bioessays. 2000;22(2):124–37.

Jumper J, Evans R, Pritzel A, Green T, Figurnov M, Ronneberger O, et al. Highly accurate protein structure prediction with AlphaFold. Nature. 2021;596(7873):583–9.

Jung YS, Zweckstetter M. Backbone assignment of proteins with known structure using residual dipolar couplings. J Biomol NMR. 2004;30(1):25–35.

Kilic S, Bachmann AL, Bryan LC, Fierz B. Multivalency governs HP1α association dynamics with the silent chromatin state. Nat Commun. 2015;6:7313.

Larson AG, Elnatan D, Keenen MM, Trnka MJ, Johnston JB, Burlingame AL, et al. Liquid droplet formation by HP1α suggests a role for phase separation in heterochromatin. Nature. 2017;547(7662):236–40.

Lipsitz RS, Tjandra N. Residual dipolar couplings in NMR structure analysis. Annu Rev Biophys Biomol Struct. 2004;33:387–413.

Mirdita M, Schutze K, Moriwaki Y, Heo L, Ovchinnikov S, Steinegger M. ColabFold: making protein folding accessible to all. Nat Methods. 2022;19(6):679–82.

Mishima Y, Watanabe M, Kawakami T, Jayasinghe CD, Otani J, Kikugawa Y, et al. Hinge and chromoshadow of HP1α participate in recognition of K9 methylated histone H3 in nucleosomes. J Mol Biol. 2013;425(1):54–70.

Munari F, Rezaei-Ghaleh N, Xiang S, Fischle W, Zweckstetter M. Structural plasticity in human heterochromatin protein 1β. PLoS One. 2013;8(4):e60887.

Munari F, Soeroes S, Zenn HM, Schomburg A, Kost N, Schroder S, et al. Methylation of lysine 9 in histone H3 directs alternative modes of highly dynamic interaction of heterochromatin protein hHP1β with the nucleosome. J Biol Chem. 2012;287(40):33756–65.

Nishibuchi G, Machida S, Osakabe A, Murakoshi H, Hiragami-Hamada K, Nakagawa R, et al. N-terminal phosphorylation of HP1α increases its nucleosome-binding specificity. Nucleic Acids Res. 2014;42(20):12498–511.

Phan TM, Kim YC, Debelouchina GT, Mittal J. Interplay between charge distribution and DNA in shaping HP1 paralog phase separation and localization. eLife. 2023;12:RP90820. https://doi.org/10.1101/2023.05.28.542535

Shen Y, Delaglio F, Cornilescu G, Bax A. TALOS+: a hybrid method for predicting protein backbone torsion angles from NMR chemical shifts. J Biomol NMR. 2009;44(4):213–23.

Smothers JF, Henikoff S. The hinge and chromo shadow domain impart distinct targeting of HP1-like proteins. Mol Cell Biol. 2001;21(7):2555–69.

Ukmar-Godec T, Cima-Omori MS, Yerkesh Z, Eswara K, Yu T, Ramesh R, et al. Multimodal interactions drive chromatin phase separation and compaction. Proc Natl Acad Sci USA. 2023;120(50):e2308858120.

Vakoc CR, Mandat SA, Olenchock BA, Blobel GA. Histone H3 lysine 9 methylation and HP1gamma are associated with transcription elongation through mammalian chromatin. Mol Cell. 2005;19(3):381–91.

Varadi M, Anyango S, Deshpande M, Nair S, Natassia C, Yordanova G, et al. AlphaFold protein structure database: massively expanding the structural coverage of protein-sequence space with high-accuracy models. Nucleic Acids Res. 2022;50(D1):D439–44.

Zeng W, Ball AR Jr, Yokomori K. HP1: heterochromatin binding proteins working the genome. Epigenetics. 2010;5(4):287–92.

Zweckstetter M. NMR: prediction of molecular alignment from structure using the PALES software. Nat Protoc. 2008;3(4):679–90.

Zweckstetter M, Bax A. Evaluation of uncertainty in alignment tensors obtained from dipolar couplings. J Biomol NMR. 2002; 23(2):127–37.

## SUPPORTING INFORMATION

Additional supporting information can be found online in the Supporting Information section at the end of this article.

**How to cite this article:** Ukmar-Godec T, Yu T, de Opakua AI, Pantoja CF, Munari F, Zweckstetter M. Conformational diversity of human HP1α. Protein Science. 2024;33(7):e5079. https://doi.org/10.1002/pro.5079